

SIMULATED VOLCANIC ASH SATELLITE IMAGERY

Sarah Millington⁽¹⁾, Roger Saunders⁽¹⁾, Peter Francis⁽¹⁾, Michael Cooke⁽¹⁾, Frances Beckett⁽¹⁾, John Stevenson⁽²⁾

⁽¹⁾ Met Office, FitzRoy Road, Exeter, EX1 3PB, UK, Email: sarah.millington@metoffice.gov.uk

⁽²⁾ School of Geosciences, The University of Edinburgh, West Mains Road, Edinburgh, EH9 3JW, Scotland

ABSTRACT

Spinning Enhanced Visible and Infrared Radiometer (SEVIRI) volcanic ash images have been simulated using dispersion model volcanic ash concentration forecasts and numerical weather prediction data in a radiative transfer model. The purpose of the simulated images is to compare them to the equivalent images derived from the observed data in order to assess the quality of the dispersion model ash forecast. The volcanic ash signal in the images is sensitive to a number of factors including ash particle size distribution (PSD). The effect of different PSDs and the reduced sensitivity of infrared data to large ash particles are studied. If the volcanic cloud contains a significant proportion of large ash particles the mass retrieved from observed data may be severely underestimated.

1. VOLCANIC ASH ADVISORY CENTRES

Airborne volcanic ash poses a significant hazard to aviation due to the possibility of ingestion of ash into jet engines and the abrasive nature of ash particles [1]. Consequently Volcanic Ash Advisory Centres (VAACs) were established to advise the aviation industry on the presence of volcanic ash in the atmosphere. There are nine VAACs around the world, each with their area of responsibility (Fig. 1). In Europe, the London VAAC (at the UK Met Office) issues advisories about ash in the north-east Atlantic, Iceland, British Isles and Arctic area and the Toulouse VAAC (at Météo-France) issues advisories for the rest of Europe, central Asia and Africa. The International Civil Aviation Organisation (ICAO) sets out procedures for the operations of VAACs.

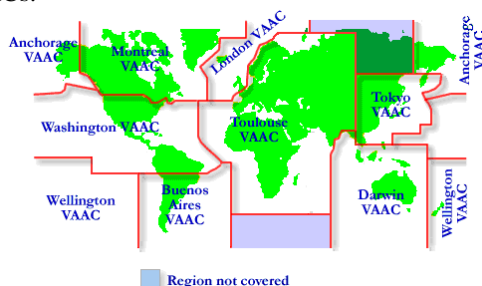


Figure 1. Areas of responsibility of the world's nine Volcanic Ash Advisory Centres

Satellite imagery is a key tool in monitoring volcanic ash over the large areas of responsibility. Along with other information, particularly from local observations

of the eruption, the data are used to inform the source term for the running of an atmospheric dispersion model and to assess the quality of the ash forecasts produced. The simulated imagery enables model forecasts and observed satellite data to be compared on a like-by-like basis. An additional benefit of the simulated imagery is to enable the study of factors that affect observed satellite data. All these data contribute to the information needed to produce Volcanic Ash Advisory Statements in text and graphic forms (Fig. 2).

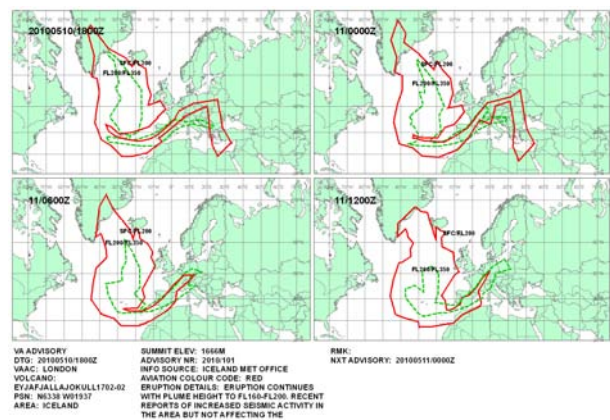


Figure 2. Example of a Volcanic Ash Advisory Statement graphic from the London VAAC

2. SATELLITE DATA

At the UK Met Office (London VAAC), satellite data from the Spinning Enhanced Visible and Infrared Radiometer (SEVIRI) are used to identify ash-contaminated areas. SEVIRI operates on Meteosat Second Generation (MSG) geostationary satellite at 0° latitude. It has 12 channels in the visible and infrared. Here, infrared channels with a sub-satellite point resolution of 3 km are used so that ash is monitored day and night. SEVIRI scans the full-earth disk every 15 minutes providing good temporal coverage for monitoring the dispersion of ash.

To detect ash-contaminated areas a series of threshold tests are carried out using SEVIRI data from the 8.7, 10.8 and 12.0 μm channels [2]. Retrievals are performed in the areas identified as being ash contaminated using SEVIRI data to estimate the column mass loading, the effective radius of the ash particles and the ash cloud pressure (height). Reference [2] used a 1D-Var approach to estimate ash properties that optimally fit the

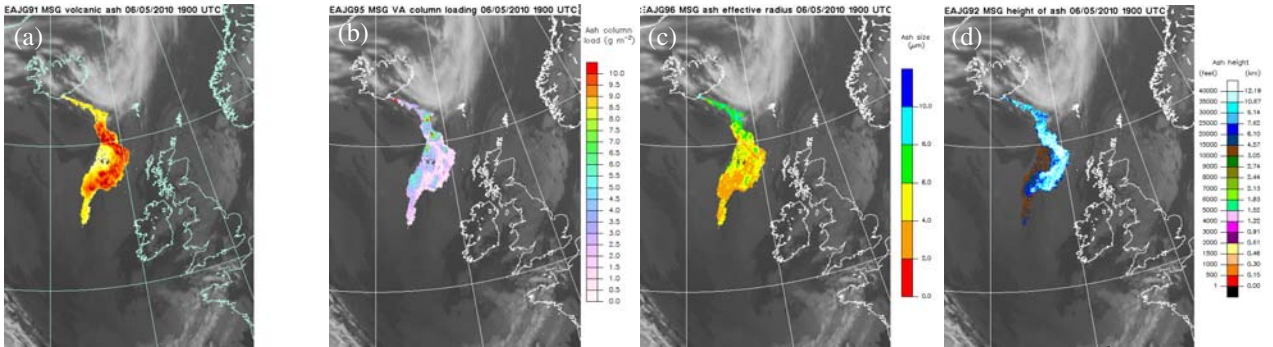


Figure 3. SEVIRI ash detection and retrieval images for Eyjafjallajökull eruption at 12 UTC on 6th May 2010. (a) is the ash detection images with the colours showing the BT10.8 – BT12.0 value, (b), (c) and (d) are retrievals of mass column loading, ash particle effective radius and height of the ash cloud respectively.

observed SEVIRI data (Fig. 3). In this technique (implemented at the Met Office) data from SEVIRI channels centred at 10.8, 12.0 and 13.4 μm are used.

In addition to the automated detection and retrievals, SEVIRI images are produced every 15 minutes for subjective interpretation (Fig. 6). The brightness temperature difference between the 10.8 and 12.0 μm channels (BT10.8 – BT12.0) exploits the so-called “reverse absorption” properties of volcanic ash [3] where ash tends to be more absorbing at 10.8 μm than at 12.0 μm leading to negative values whilst ice and water clouds tend to produce positive values. This technique is widely used and forms the basis for some of the automated ash detection tests mentioned above. These images can contain many negative values not caused by ash and so require careful interpretation (e.g. low-level water clouds, temperature inversions). The second type of image is the so-called dust RGB (red-green-blue). This was developed by EUMETSAT and provides excellent animations 24 hours a day to view ash dispersion. The BT12.0 – BT10.8 data are assigned to the red channel, BT8.7 – BT10.8 to the green channel and BT10.8 to the blue channel (see [2] for details).

The forecasters compiling the advisory statements use ash forecasts from the dispersion model, retrievals of ash physical properties, SEVIRI imagery, data from other satellites (e.g. MODIS, AVHRR, IASI, OMI, GOME-2) and other sources (e.g. radar, aircraft reports, lidar).

3. METHOD TO SIMULATE IMAGERY

In order to simulate volcanic ash imagery some properties of the ash must be assumed, namely the refractive indices and the particle size distribution. These are used to calculate the absorption and scattering coefficients using Mie theory. The coefficients are used in a radiative transfer model with input data from an atmospheric dispersion and numerical prediction models to simulate SEVIRI infrared brightness temperatures.

3.1. Refractive indices

The refractive indices depend on the composition of the ash particles. This is generally unknown at the onset of an eruption. Published data (Fig. 4) includes refractive indices for andesite and obsidian [4], volcanic dust [5] and mineral dust [6]. Refractive indices for a sample of Eyjafjallajökull ash have recently been derived (D. Peters, personal communication) and were found to be similar, over SEVIRI infrared wavelengths, to andesite ash as published by [4]. Reference [7] shows the error that can occur from assumption of inappropriate refractive indices.

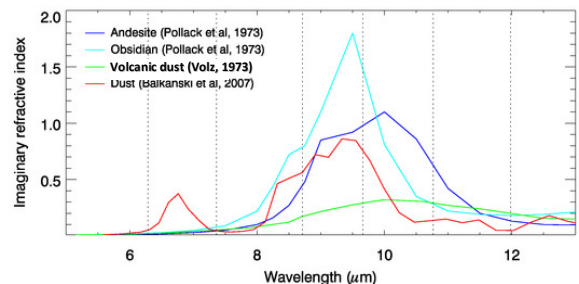


Figure 4. Imaginary refractive indices for volcanic ash and mineral dust over the SEVIRI infrared channels (central wavelengths shown by dotted lines)

The imaginary refractive indices in Fig. 4 are an indication of the absorption properties of the particles and show the “reverse absorption” effect of ash/dust, i.e. greater absorption at 10.8 μm than at 12.0 μm . The variation in the gradient between 10.8 μm and 12.0 μm between the different compositions indicates that the strength of the BT10.8 – BT12.0 signal can vary between different ash types.

Reference [8] found that andesite ash refractive indices were most appropriate for the Eyjafjallajökull eruption. Along with recent evidence for the similarity of the refractive indices with those for an Eyjafjallajökull ash sample it was decided to use andesite refractive indices throughout this study.

3.2. Particle size distribution

The particle size distribution (PSD) is used along with the refractive indices to calculate the absorption and scattering coefficients. Reference [8] found the sensitivity of the volcanic ash signal to be greater to the PSD than to the refractive indices. Again, the PSD is unknown at the time of an eruption and is difficult to measure accurately due to limitations with collection and measurement techniques (e.g. larger particles shattering on collection). However, PSD for airborne ash have been measured using instrumentation on aircraft. Reference [9] found that a lognormal distribution with a median radius of 1.9 μm and a standard deviation of 1.85 best fitted the ash particle size observations made of the Eyjafjallajökull ash on the FAAM aircraft (Facility for Airborne Atmospheric Measurements) during May 2010. Other observations, such as those of the Mt. Redoubt ash in 1990 [10], also fit a lognormal size distribution. The PSD for the Mt. Redoubt ash was found to have a median radius of 0.8 μm and a standard deviation of 2.0 [10]. A lognormal distribution takes the form:

$$n(r) = \frac{N_0}{\sqrt{2\pi}} \frac{1}{\ln(\sigma)} \frac{1}{r} \exp\left(-\frac{(\ln r - \ln r_m)^2}{2 \ln^2(\sigma)}\right) \quad (1)$$

where N_0 is the total number density, r is the particle radius, r_m is the median radius of the PSD and σ is the standard deviation of the PSD (Fig. 5).

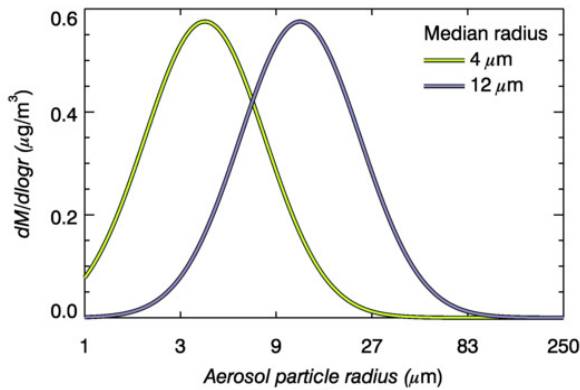


Figure 5. Example lognormal particle size distributions with a standard deviation of 2.0 and median radii of 4 μm (green) and 12 μm (blue)

Reference [8] found that the volcanic ash signal in simulated imagery was strongly dependant on the particle size distribution assumed, thus the sensitivity to this ash property is studied here.

3.3. Radiative transfer modelling

The fast radiative transfer model RTTOV was used to forward model the SEVIRI radiances using Numerical

Prediction Weather (NWP) data from the Met Office's Global version of the Unified Model [11] and atmospheric dispersion model data. RTTOV is a very fast radiative transfer model for nadir viewing passive infrared and microwave satellite radiometers, spectrometers and interferometers. RTTOV-10 was used in this study [12]. The aerosol multiple scattering is parameterized by scaling the layer optical depth by a factor derived by including the backward scattering in the emission of a layer and in the transmission between levels (a scaling approximation) [13]. The absorption and scattering coefficients calculated using Mie theory are needed by RTTOV to simulate the effect of the ash on the infrared radiances.

The ash concentration data are from NAME (Numerical Atmospheric dispersion Modelling Environment) [14]. These data are converted to aerosol number density and interpolated onto the NWP grid for input to RTTOV. NWP temperature and humidity data from the Met Office's global version of the Unified Model are used as input to RTTOV along with the aerosol number density. Using the absorption and scattering coefficients RTTOV forward models the radiances for SEVIRI. The outputs are converted to brightness temperatures and used to create BT10.8 – BT12.0 and dust RGB images in the same way as done with observed brightness temperatures.

3.4. Example: 7th May 2010

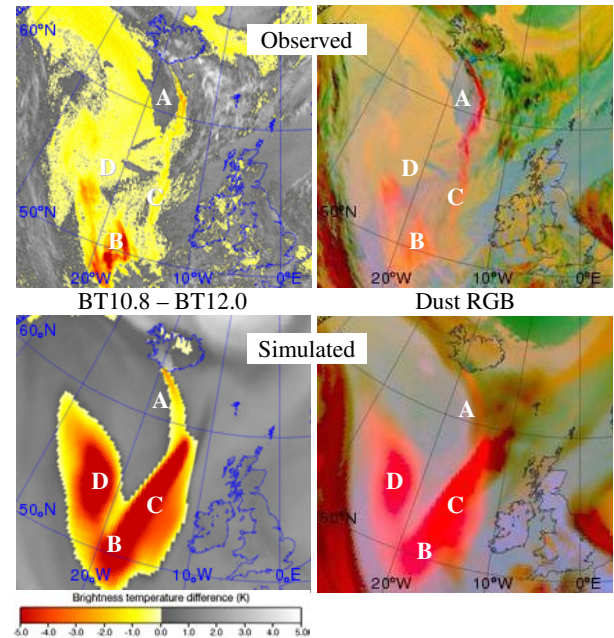


Figure 6. Observed and simulated SEVIRI BT10.8 – BT12.0 and dust RGB at 12 UTC on 7th May 2010. Images were simulated using andesite refractive indices and a PSD with median radius of 4 μm and standard deviation of 2.0 (green line in Fig. 5). The letters label areas discussed in the text.

Fig. 6 shows examples of observed and simulated BT10.8 – BT12.0 and dust RGB images during the Eyjafjallajökull eruption at 12 UTC on 7th May 2010. Eyjafjallajökull started eruption on 23rd March 2010 with increased intensity on 14th April leading to wide-scale airspace closures over Europe. Following a decrease in activity in the latter part of April the eruption intensity increased on 5th/6th May 2010. Fig. 6 shows an ash plume extending southwards from Iceland over the Atlantic to the west of the British Isles.

The observed BT10.8 – BT12.0 shows a strong volcanic ash signal close to Iceland at location A in Fig.6 (orange colours with values of approx. -3 K) and a large area to the west of Ireland at location B (values of -2 to -5 K). The dust RGB has strong pink/red colours at A, but orange colours at B. These signals can be explained by the ash particles being larger at location A than B, which is likely to be the case since one would expect larger particles near the volcano. As particle size decreases the absorption coefficient at 8.7 μm increases (relative to that at 10.8 μm) resulting in a larger green component in the dust RGB image, hence the orange colour. As will be shown below smaller ash particles produce a stronger ash signal in the BT10.8 – BT12.0 for the same mass loading; this corresponds to the strong signal at B. The variability in the signals observed along the length of the plume may be due to varying particle size, ash concentration, ash composition, sulphur dioxide concentration, water vapour, sea/ground surface temperature, atmospheric factors or, most likely, a combination of these factors.

The simulated images show a weak ash signal directly to the south of Iceland (location A) with strong signals to the west of the British Isles (locations B, C and D). This could indicate that the NAME forecast ash concentrations are too low at location A and too high at locations C and D. This could occur due to timing error in the change in ash emission rate from the volcano (derived from the eruption plume height) or a number of other factors, e.g. NWP errors. An important point to note is that while many of the actual ash physical properties may change over the length of the plume (as noted above) they are fixed in the simulation, i.e. the PSD and ash composition are constant along the length of the plume. Atmospheric factors vary due to the NWP data, but no sulphur dioxide or other volcanic gases are taken into account.

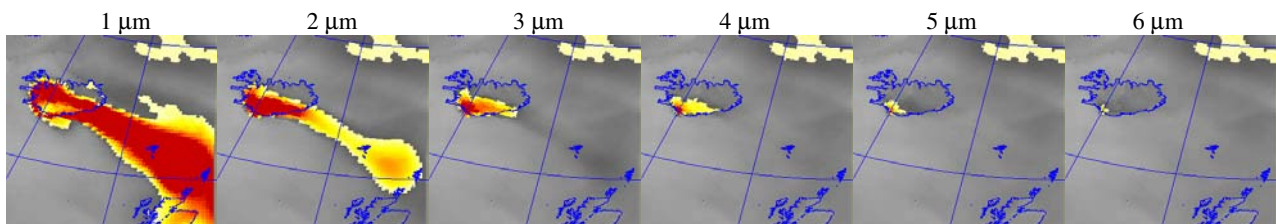


Figure 8. Simulated BT10.8 – BT12.0 images each using the same ash concentration for 17th May 2010 but with particle radius varying from 1 – 6 μm (key same as in Fig. 6).

4. SENSITIVITY TO ASH PARTICLE SIZE

To calculate the absorption and scattering coefficients needed for RTTOV and the aerosol number density from the ash concentration a PSD is needed. In order to study the sensitivity of the resulting volcanic ash signals PSDs with a standard deviation (σ) of 1.0001 and different median radii were used in the simulations. The PSD are so narrow that effectively the particles are all a single size, i.e. the size of the median radius.

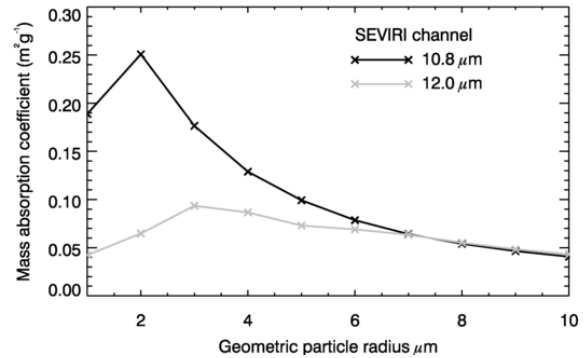


Figure 7. Mass absorption coefficient for andesite ash particles.

The mass absorption coefficient is plotted in Fig. 7 for the 10.8 μm and 12.0 μm SEVIRI channels for andesite ash particles varying in size from 1 to 10 μm . The mass absorption coefficient is the effective cross-sectional area per unit mass of particles that absorbs energy. Fig. 7 shows the “reverse absorption” properties characteristic of ash for particles with radii less than 7 μm ; here the mass absorption coefficient is greater at 10.8 μm than at 12.0 μm . For particles larger than 7 μm radius the negative BT10.8 – BT12.0 would not be expected and therefore many ash detection and retrieval methods would fail. Thus, we can conclude that the SEVIRI reverse absorption ash detection method is only sensitive to particles with radii less than 7 μm .

Fig. 8 shows the effect of the decreasing sensitivity of the BT10.8 – BT12.0 ash signal with increasing particle size. When the particles have radii of 6 μm only the areas of volcanic ash at the volcano produces a volcanic ash signal (i.e. where the concentration of ash is greatest). The ash concentration is the same for all the simulations in Fig. 8 and thus it illustrates the danger of not detecting large ash particles using this methodology.

Of course, real ash clouds have a distribution of particle sizes. Reference [15] shows that large volcanic ash particles ($> 20 \mu\text{m}$) can travel large distances and that it should not be assumed that they fall out close to the volcano. The consequence of this is that a large proportion of mass may be missed by satellite retrievals from observed infrared data due to the lack of sensitivity to these large particles. This is discussed further in [15].

5. SUMMARY

Volcanic ash imagery has been simulated using ash concentration data from an atmospheric dispersion model and NWP data. The ash absorption and scattering coefficients needed for the radiative transfer modelling were calculated from Mie theory using assumptions about the ash refractive indices and particle size distribution. The resulting simulated SEVIRI imagery can be compared to equivalent imagery generated from observed data and is a useful tool for forecasters to use to identify errors in the ash forecasts.

The volcanic ash signal in the simulated BT10.8 – BT12.0 and dust RGB imagery is particularly sensitive to the assumed particle size distribution. It has been shown that SEVIRI (or similar) BT10.8 – BT12.0 imagery is only sensitive to ash particles with radii of less than $7 \mu\text{m}$. Larger particles do not exhibit the classic “reverse absorption” signature of volcanic ash. As a result large particles in a volcanic ash cloud may go undetected and consequently the spatial coverage of the ash and the mass loading may be underestimated.

6. REFERENCES

1. Casadevall, T.J., ed. (1994). Volcanic ash and aviation safety: *Proceedings of the First International Symposium on Volcanic Ash and Aviation Safety*. Vol. 2047. DIANE Publishing.
2. Francis, P. N., Cooke, M. C., & Saunders, R. W. (2012). Retrieval of physical properties of volcanic ash using Meteosat: A case study from the 2010 Eyjafjallajökull eruption. *Journal of Geophysical Research: Atmospheres*, **117**.
3. Prata, F. (1989), Observations of volcanic ash clouds in the 10–12 mm window using AVHRR/2 data, *Int. J. Remote Sens.*, **10**, 751–761, doi:10.1080/01431168908903916.
4. Pollack, J. B., O. B. Toon, and B. N. Khare (1973), Optical properties of some terrestrial rocks and minerals, *Icarus*, **19**, 372–389, doi:10.1016/0019-1035(73)90115-2.
5. Volz, F. E. (1973), Infrared optical constants of ammonium sulfate, Sahara dust, volcanic pumice, and flyash, *Appl. Opt.*, **12**(3), 564–568, doi:10.1364/AO.12.000564.
6. Balkanski, Y., M. Schulz, T. Claquin, and S. Guibert (2007), Reevaluation of mineral aerosol radiative forcings suggests a better agreement with satellite and AERONET data, *Atmos. Chem. Phys.*, **7**, 81–95, doi:10.5194/acp-7-81-2007.
7. Mackie, S., Millington, S.C. & I.M. Watson (2013), How Assumed Composition Affects The Interpretation of Satellite Observations of Volcanic Ash. *In preparation*.
8. Millington, S. C., Saunders, R. W., Francis, P. N., & Webster, H. N. (2012), Simulated volcanic ash imagery: A method to compare NAME ash concentration forecasts with SEVIRI imagery for the Eyjafjallajökull eruption in 2010. *Journal of Geophysical Research: Atmospheres*, **117**.
9. Johnson, B., Turnbull, K., Brown, P., ... & Rosenberg, P. (2012). In situ observations of volcanic ash clouds from the FAAM aircraft during the eruption of Eyjafjallajökull in 2010. *Journal of Geophysical Research*, **117**.
10. Hobbs, P. V., Radke, L. F., Lyons, J. H., Ferek, R. J., Coffman, D. J., & Casadevall, T. J. (1991). Airborne measurements of particle and gas emissions from the 1990 volcanic eruptions of Mount Redoubt. *Journal of Geophysical Research*, **96**, 18735-18752.
11. Davies, T., Cullen, M. J. P., Malcolm, A. J., Mawson, M. H., Staniforth, A., White, A. A., & Wood, N. (2005). A new dynamical core for the Met Office's global and regional modelling of the atmosphere. *Quarterly Journal of the Royal Meteorological Society*, **131**, 1759-1782.
12. NWPSAF website: <http://research.metoffice.gov.uk/research/interproj/nwpsaf/>
13. Matricardi M. (2005). The inclusion of aerosols and clouds in RTIASI, the ECMWF fast radiative transfer model for the infrared atmospheric sounding interferometer. "Technical Memorandum" 474, ECMWF, available at: <http://www.ecmwf.int/publications/library/reference/s/list/14>
14. Jones, A., Thomson, D., Hort, M. & Devenish, B., (2006). The U.K. Met Office's Next-Generation Atmospheric Dispersion Model, NAME III. In: Borrego C, Norman AL (eds) *Air Pollution Modeling and Its Application XVII*, Springer US, Boston, MA.
15. Stevenson, J.A., Millington, S.C., Beckett, F., Swindles G.T. & T. Thordarson. (2013). Giant aerosol particles of extremely fine volcanic ash travel long distances: implications for remote sensing data. *In preparation*.